Low mass AGB stellar models for $0.003 \le Z \le 0.02$: basic formulae for nucleosynthesis calculations

O. Straniero[1], I. Domínguez[2], S. Cristallo[3], R. Gallino[4]

[1] INAF, Osservatorio Astronomico di Teramo, Italy
straniero@te.astro.it

[2] Universidad de Granada, Spain
inma@ugr.es

[3] INAF, Osservatorio Astronomico di Teramo, Italy
cristallo@te.astro.it

[4] Dip. Fisica Generale Università di Torino and Sez. INFN Torino, Italy
gallino@ph.unito.it

Abstract

We have extended our published set of low mass AGB stellar models to lower metallicity. Different mass loss rates have been explored. Interpolation formulae for luminosity, effective temperature, core mass, mass of dredge up material and maximum temperature in the convective zone generated by thermal pulses are provided. Finally, we discuss the modifications of these quantities as obtained when an appropriate treatment of the inward propagation of the convective instability, caused by the steep rise of the radiative opacity occurring when the convective envelope penetrates the H-depleted region, is taken into account.

Keywords stars: AGB, evolution, nucleosynthesis, abundances

1 Introduction.

Results from detailed AGB stellar models demonstrate that low mass AGB stars (i.e. $1.3 \le M/M_\odot \le 3$) are the producers of the main component of the cosmic s-elements (Straniero et al. 1995; Gallino et al. 1998; Busso et al. 1999). Such a scenario has been confirmed by the measurements of the chemical composition of AGB stars (Lambert et al. 1995; Busso et al. 2001; Abia et al. 2001,2002) and by the analysis of the isotopic composition of meteoritic SiC grains (Gallino et al. 1997).

The present generation of AGB stars, as observed in the disk of our Galaxy, have a nearly solar chemical composition. However, SiC grains found in pristine meteorites

originated in the C-rich circumstellar envelope of a pre-solar generation of AGB stars, whose original metallicity could have been somewhat lower than that found in the solar system material. In addition, an important contribution to our understanding of AGB stars comes from observations of the stellar population in the fields of the Small and the Large Magellanic Clouds, whose average metallicities are about 1/5 and 1/2 of the solar, respectively. In a previous paper (Straniero et al. 1997) the properties of low mass AGB stellar models with solar composition have been extensively discussed. Here we present an extension of these models to lower metallicity.

2 The grid of models and interpolations.

The full grid of models is summarized in Tab. 1. The corresponding AGB evolutionary sequences have been obtained by means of the FRANEC code, the same described in Straniero et al. (1997). The initial mass, the helium content and the metallicity are reported in column 1, 2 and 3, respectively. Various mass loss rates have been applied during the AGB phase. In all cases, we have used the Reimers formula (Reimers, 1975):

$$\dot{M}(M_\odot/yr) = 1.34 \cdot 10^{-5} \cdot \eta \cdot \frac{L^{\frac{3}{2}}}{M \cdot T_{eff}^2}$$

where M and L are in solar units and η is a free parameter (see fourth column in Tab. 1). We have not considered mass loss in pre-AGB evolution, since, in the mass range 1.5-3 $M_\odot$, just a few hundredths of solar masses are expected to be lost. For example, by adopting η=0.4 as representative of the pre-AGB mass loss rate (e.g. Fusi Pecci & Renzini 1976), we found that the total mass lost before the onset of the AGB phase by a 2 $M_\odot$ star with solar composition should be 0.04 $M_\odot$. Clearly, such a small amount of mass loss has negligible consequences on the pre-AGB evolution.

The thermally pulsing AGB models (TP-AGB) are characterized by three distinct phases:

1) The *early phase*. It includes the first few (gentle) thermal pulses which are not followed by the third dredge up (TDU);

2) The *TDU phase*. It begins when the mass of the H exhausted core becomes as large as $0.59 - 0.6 M_\odot$. The amount of mass dredged up firstly increases, as the core mass increases, and then decreases, when the envelope mass is substantially reduced;

3) The *final phase*. During the last part of the AGB, the concurrent actions of mass loss and H-burning erode the envelope mass and the TDU ceases. The minimum envelope mass for the occurrence of the TDU is about $0.4 - 0.5 M_\odot$.

The variation of the mass dredged up, as a function of the core mass, is shown in Fig. 1 for some selected sequences of models.

An interpolation on the grid of models provides useful analytic expressions for relevant quantities, as a function of $M_{\rm H}$ (the mass of the H-exhausted core, in $M_\odot$), M_{env} (the mass of the H-rich envelope, in $M_\odot$) and Z (the initial mass fraction of elements with $A \geq 12$).

In the following we report the result of these interpolations.

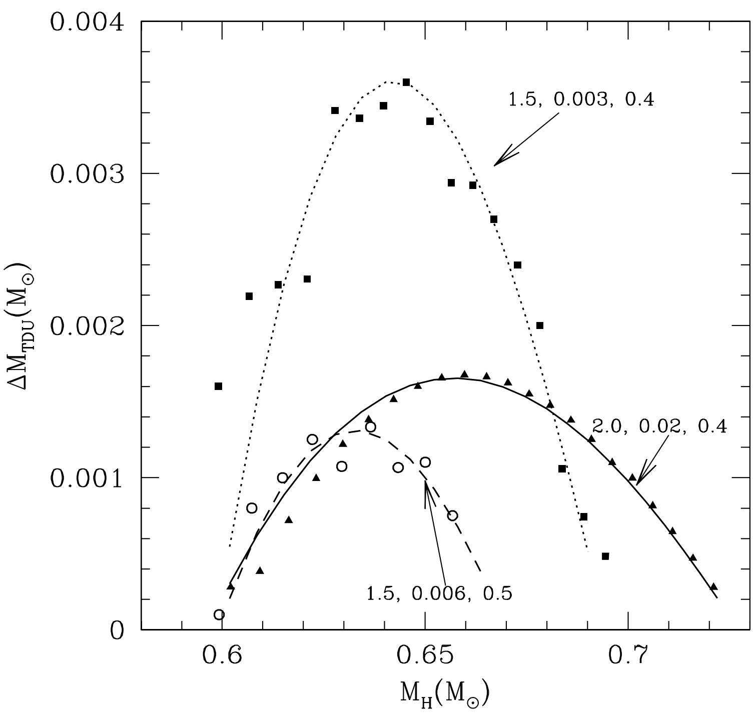

Figure 1: The amount of mass dredged up per thermal pulse for three evolutionary sequences: $M = 2.0\ M_\odot$, $Z = 0.02$ and $\eta = 0.4$ - triangles (FRANEC models) and solid line (interpolation formula); $M = 1.5\ M_\odot$, $Z = 0.006$ and $\eta = 0.5$ - circles (FRANEC models) and dashed line (interpolation formula); $M = 1.5\ M_\odot$, $Z = 0.003$ and $\eta = 0.4$ - squares (FRANEC models) and dotted line (interpolation formula).

1. The time elapsed between two successive thermal pulses (interpulse period):

$$\Delta t_{ip}(10^5 \mathrm{yr}) = 18.5178 - 59.8876 \cdot M_{\mathrm{H}} + 48.8462 \cdot M_{\mathrm{H}}^2 - 4.0273 \cdot \log Z +$$

$$+5.8422 \cdot M_{\mathrm{H}} \cdot \log Z$$

which is valid for $M_{\mathrm{H}} \geq 0.58$. For smaller core masses, substitute M_{H} with $(1.16 - M_{\mathrm{H}})$. The standard deviation of this fit (i.e. the average difference between the values calculated with the fitting formula and those of the models) is 0.01.

2. The mass of the H-depleted material dredged up in a given TDU episode:

$$\Delta M_{TDU}(M_{\odot}) = (1.0 + 0.21 \cdot \log \tfrac{Z}{Z_{\odot}} + 6.3 \cdot (\log \tfrac{Z}{Z_{\odot}})^2)(-6.2 \cdot 10^{-4} +$$

$$+9.1 \cdot 10^{-4} \cdot M_{env} - 3.7 \cdot 10^{-4} \cdot M_{env}^2 + 5.061 \cdot 10^{-2} \cdot M_{env} \cdot \delta M_{\mathrm{H}} -$$

$$-5.96 \cdot 10^{-3} \cdot M_{env}^2 \cdot \delta M_{\mathrm{H}} - 3.8372 \cdot 10^{-1} \cdot M_{env} \cdot \delta M_{\mathrm{H}}^2 + 9.448 \cdot 10^{-2} \cdot M_{env}^2 \cdot \delta M_{\mathrm{H}}^2)$$

where $Z_{\odot} = 0.02$ and $\delta M_{\mathrm{H}} = M_{\mathrm{H}} - M_{\mathrm{H}}^*$ and M_{H}^* is the core mass at the last thermal pulse without TDU (last pulse of the *early phase*). For the masses and chemical compositions we have considered, M_{H}^* ranges between 0.59 and 0.6. The curves reported in Fig. 1 have been obtained by using $M_{\mathrm{H}}^* = 0.595$. When $M_{env} < 0.4$ or $\delta M_{\mathrm{H}} \leq 0$, take $\Delta M_{TDU} = 0$. The standard deviation of this fitting formula is $2 \cdot 10^{-4}$.

3) The luminosity at half of the interpulse period:

$$\log \tfrac{L}{L_{\odot}} = 3.603 + 6.7806 \cdot \Delta M_{\mathrm{H}} - 27.582 \cdot \Delta M_{\mathrm{H}}^2 + 277.333 \cdot \Delta M_{\mathrm{H}}^4$$

here $\Delta M_{\mathrm{H}} = M_{\mathrm{H}} - M_{\mathrm{H}}(t_0)$ and $M_{\mathrm{H}}(t_0)$ is the core mass at the epoch of the first thermal pulse (t_0). The latter quantity slightly depends on the metallicity: $M_{\mathrm{H}}(t_0) = 0.517 - 1.93910^{-2} \times \log Z$. For this fit the standard deviation is 10^{-4}.

4) The effective temperature at half of the interpulse period:

$$\log T_{eff}(K) = 5.0475 + 0.1438 \cdot \log Z_{eff} + 0.0513 \cdot (\log Z_{eff})^2 - 4.1895 \cdot M_{\mathrm{H}} + 2.9594 \cdot M_{\mathrm{H}}^2$$

here, Z_{eff} is the effective metallicity, which includes the extra-carbon in the envelope due to the third dredge up. The use of Z_{eff}, instead of Z, has minor effects on solar composition stars, but may significantly increase the estimated radius and, in turn, the mass loss rate for stars with an original low content of metal. The standard deviation is $5 \cdot 10^{-4}$.

5) The maximum temperature attained at the bottom of the convective zone generated by a thermal pulse:

$$\log T_{max}(K) = 6.7747 + 4.6856 \cdot M_{\mathrm{H}} - 3.21 \cdot M_{\mathrm{H}}^2 + 0.01 \cdot M_{env} +$$

$$-6.2337 \cdot Z + 7.87595 \cdot Z \cdot M_{\mathrm{H}}$$

for $\log T_{max}$ the standard deviation is $3 \cdot 10^{-3}$. Finally, the evolution of the core mass during the whole TP-AGB phase may be estimated by means of the following formula:

$$M_{\rm H} = M_{\rm H}^{*} + 6.9 \cdot 10^{-3} \cdot k - 6.0 \cdot 10^{-5} \cdot k^2$$

where $k = -n, -n+1, ..., 0, 1, ..., j$. $k = 0$ corresponds to the last thermal pulse without TDU ($M_{\rm H} = M_{\rm H}^{*}$); $n+1$ is the number of TPs of the *early phase*, while j is the number of TPs occurred from the first TDU episode up to the AGB tip (*TDU phase + final phase*). This formula gives $M_{\rm H}$ within $5 \cdot 10^{-3}$ $M_{\odot}$. Then, the envelope mass is easily obtained: $M_{env} = M - M_{\rm H}$, where M is the total mass.

Note that, if the initial mass of the star is too small, the conditions for the activation of the third dredge up (namely, $M_{\rm H} \geq 0.60$ $M_{\odot}$ and $M_{env} \geq 0.4$ $M_{\odot}$) are never reached. The minimum mass for the occurrence of the TDU, as a function of the mass loss rate, are reported in Fig. 2, for solar composition models. In stars with masses exceeding this lower limit, the envelope composition is modified by the TDU: ^{12}C and *s*-elements are enhanced. Obviously, a C-star may form, after a suitable number of TDU episodes, only if the initial mass is large enough. The dashed line in Fig. 2 shows, for solar metallicity models, the lower mass limit for the formation of a C-star as a function of η.

Both these lower limits depend on metallicity: the smaller the metallicity, the smaller is the mass for the activation of the TDU phase and the lower is the minimum initial mass for the formation of a C-star. This occurrence is illustrated in Fig. 3 (for η=0.5).

At low metallicity (i.e. $Z < 4 \cdot 10^{-3}$), even taking into account an enhanchement of the α-elements (as typically found in halo stars), the amount of oxygen in the envelope is so low that just one TDU episode is sufficient to increase the C/O ratio above unity. Correspondingly, the core mass and the luminosity at C/O = 1 decrease at low Z (see Fig. 4).

3 The efficiency of the third dredge up: the Opacity Induced Convection.

An He-rich zone, as the one left by the shell H-burning, has a significantly lower opacity than an H-rich zone, at the same temperature and pressure. Thus, when the innermost layer of the convective envelope (H-rich) penetrates into the region of decreasing H and increasing He (at the epoch of the TDU), the local value of the radiative opacity increases. Since the radiative gradient (∇_{rad}) is proportional to the opacity, the condition $\nabla_{rad} \gg \nabla_{ad}$ (where ∇_{ad} is the adiabatic temperature gradient) takes place at the base of the convective envelope. In this case, the internal boundary of the convective zone becomes unstable (Becker & Iben 1979; Castellani, Chieffi & Straniero 1990; Frost & Lattanzio 1996; Castellani, Marconi & Straniero 1998). In fact, even a small perturbation may increase the radiative gradient in the formally stable region, located immediately below the convective envelope, which immediately becomes

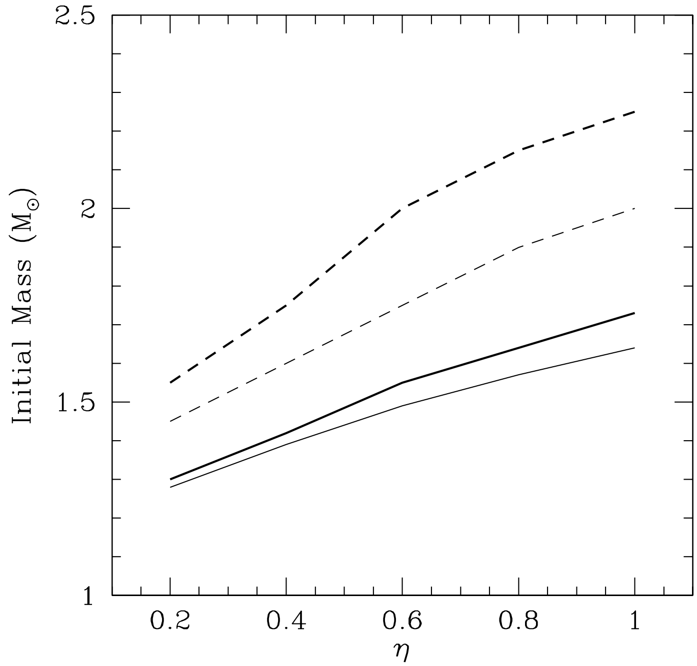

Figure 2: The minimum initial mass for the occurrence of the TDU (solid lines) and the minimum initial mass for C-star progenitors (dashed lines) as a function of the mass loss rate. The η values reported in the abscissa refer to the free parameter in the Reimers formula. These results are based on solar metallicity models ($Z = 0.02$ and $Y = 0.28$). Thick lines represent the case of models with minimal dredge up, while thin lines have been derived from models that include an exponential decline of the convective velocity at the boundaries of the convective zone (see section 3).

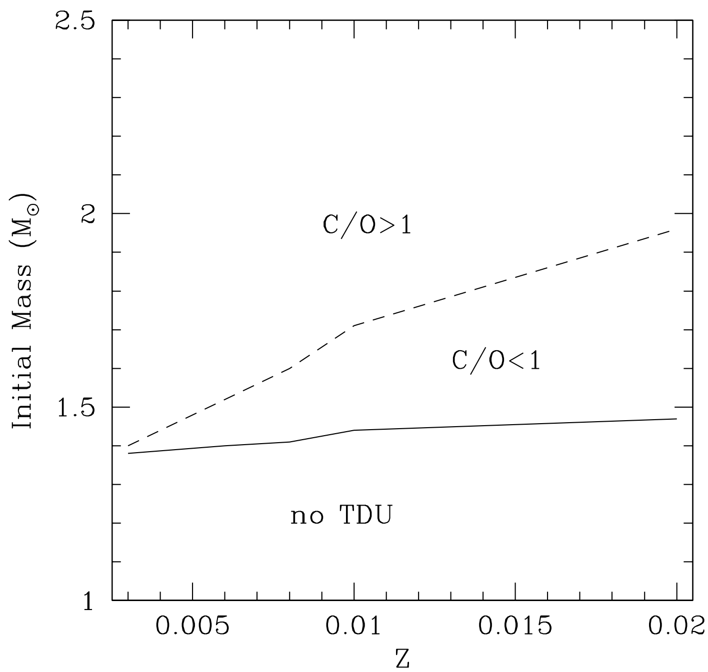

Figure 3: The minimum initial mass for the occurrence of the TDU (solid line) and the minimum initial mass for C-star progenitors (dashed line) as a function of Z. These results are based on models computed with a Reimers mass loss rate ($\eta = 0.5$) and minimal dredge up (see section 3).

M ($M_\odot$)	Y	Z	η	β
1.0	0.280	0.020	0	0
1.5	0.280	0.020	0	0
1.5	0.280	0.020	0.4	0/0.1
2.0	0.280	0.020	0.4	0/0.1
3.0	0.280	0.020	0	0
3.0	0.280	0.020	1.5	0/0.1
1.5	0.255	0.006	0.5	0/0.1
3.0	0.255	0.006	1.5	0
1.5	0.230	0.003	0.4	0/0.1
3.0	0.230	0.003	1.5	0

Table 1: The computed grid of models. M is the initial mass. Y and Z are the initial helium content and the metallicity, respectively. η is the free parameter in the Reimers mass loss formula. β is the free parameter in the exponential decline law for the boundary velocity of the convective elements (section 3).

convectively unstable. At present, a satisfactory treatment of this phenomenon has not yet been found. However, its overall effect on AGB stellar models may be derived by appling a small perturbation to the boundaries of the convective regions. As a tentative scheme, we have supposed that the velocity of the convective elements, usually evaluated by means of the mixing length theory, does not abruptly drop to 0 at the convective boundaries, but decreases following an exponential decline law (for more details on the mixing algorithm see section 2 in Chieffi et al. 2001):

$$v = v_{bce} \exp\left(-\frac{z}{\beta H_P}\right),$$

where z is the distance from the convective boundary, v_{bce} the average velocity at the convective boundary, H_P the pressure scale height at the convective boundary and β is a free parameter that controls the steepness of the velocity decline. Usually, when the convective boundary is located within a chemically homogeneous region, $v_{bce} \sim 0$ and the convective border is stable. However, at the epoch of the TDU, at the base of the convective envelope the difference between radiative and adiabatic gradients increases. Thus, v_{bce} increases, causing an inward propagation of the convective instability. The final result is a substantial increase of the TDU efficiency. With $\beta = 0.1$, for example, the amount of H-depleted mass dredged up by convection is about a factor 2 larger than that found in models without the exponential decline of the convective velocity (Cristallo et al. 2003).

Few additional models have been computed by taken $\beta = 0.1$ (see last column in Tab. 1). The effect on the minimum mass for C-star progenitors is shown in Fig. 2, in the case of solar composition models. The corresponding decrease of the minimum C-star luminosity is illustrated in Fig. 4.

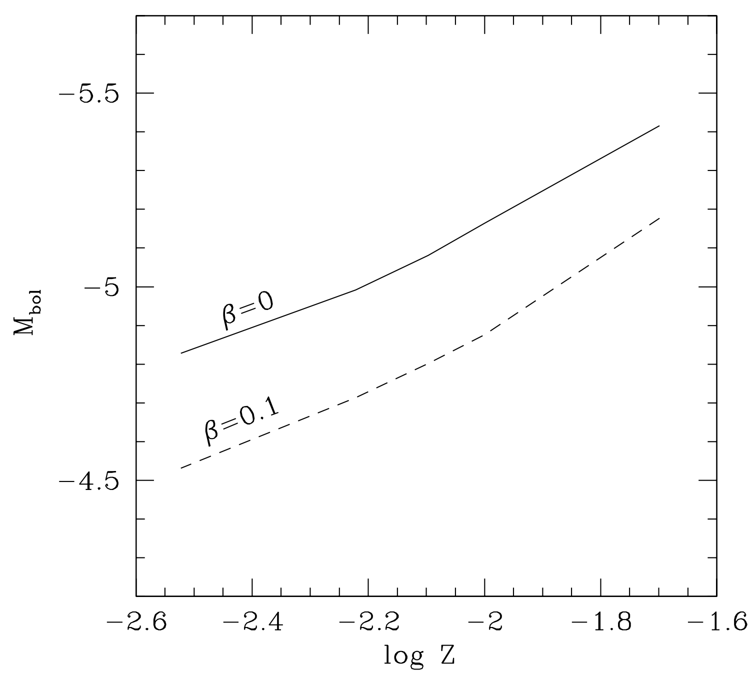

Figure 4: The minimum luminosity for a C-star as a function of Z. These results are based on models computed with a Reimers mass loss rate ($\eta = 0.5$) and with (dashed line) and without (solid line) exponential decline of the convective velocity.

4 Final remarks

In this paper, based on an homogeneous grid of low mass AGB stellar models, we provide some interpolation formulae for basic ingredients used in nucleosynthesis calculations. These formulae are strictly valid for $M \leq 3M_{\odot}$, at solar metallicity, and for $M \leq 2.5M_{\odot}$, in the metallicity range $0.003 \leq Z < 0.02$.

A study of the third dredge-up as a function of total mass and metallicity has been recently published by Karakas, Lattanzio & Pols (2002), while a comparison among the AGB stellar models computed by means of different evolutionary codes has been discussed by Lugaro et al. (2003). Once the same mass loss rate is adopted, a substantial agreement is found between our (FRANEC) results and those obtained by using the Mount Stromlo Stellar Structure Program (Frost and Lattanzio, 1996; Karakas, Lattanzio & Pols 2002).

As a final remark, note that although we have used a Reimers formula to evaluate the mass loss, since the fittings formulae are given as a function of the envelope and core masses, they can be used for any mass loss law.

Acknowledgments

This research was supported by the Italian grant MURST-FIRB, by the Spanish grant AYA2002-04094-C3-03 and by the Andalusian grant FQM-292.

References

Abia, C., Busso, M., Gallino, R., Dominguez, I., Straniero, O., & Isern, J. 2001, ApJ 559, 1117

Abia, C., Dominguez, I., Busso, M., Gallino, R., Masera, S., Straniero, O., de Laverny, P., Plez, B., & Isern, J. 2002, ApJ 579, 817

Becker, S.A., & Iben, I. Jr. 1979, ApJ 232, 831

Busso, M., Gallino, R., Lambert, D.L., Travaglio, C., & Smith, V.V. 2001, ApJ 557, 802

Busso, M., Gallino, R., & Wasserburg, G.J. 1999, ARAA 37, 239

Castellani, V., Chieffi, A., & Straniero, O. 1990, ApJS 74, 463

Castellani, V., Marconi, M., & Straniero, O., 1998, AA 340, 160

Chieffi, A., Dominguez, I., Limongi, M., & Straniero, O. 2001, ApJ 554, 1159

Cristallo, S., Gallino, R., & Straniero, O., 2003, Mem. SAIt (in press).

Frost, C., & Lattanzio, J.C. 1996, ApJ 473, 383

Fusi Pecci, F., & Renzini, A. 1976, AA 46, 447

Gallino, R., Arlandini, C., Busso, M., Lugaro, M., Travagio, C., Straniero, O., Chieffi, A., & Limongi, M. 1998, ApJ 497, 388

Gallino, R., Busso, M., & Lugaro, M. 1997, in *Astrophysical Implications of the Laboratory Study of Presolar Material*, ed. T. J. Bernatowicz and E. Zinner, *AIP Conf. Proc.*, 402, (Woodbury: American Institute of Physics), 115

Karakas, A.I., Lattanzio, & Pols, O.R. 2002, PASA 19, 515

Lambert, D.L., Smith, V.V., Busso, M., Gallino, R., & Straniero, O. 1995, ApJ 450, 302

Lugaro, M., Herwig, F., Lattanzio, J.C., Gallino, R., & Straniero, O. 2003, ApJ 586, 1305

Reimers, D. 1975, in *Problems in Stellar Atmospheres and Envelopes*, ed. B. Baschek, W.H. Kegel and G. Traving, (Berlin Springer), 229

Straniero, O., Gallino, R., Busso, M., Chieffi, A., Limongi, M., & Salaris, M. 1995, ApJ 440, L85

Straniero, O., Chieffi, A., Limongi, M., Gallino, R., Busso, M., & Arlandini, C. 1997, ApJ 478, 332